DISCRETE AND CONTINUOUS
DYNAMICAL SYSTEMS SERIES S
Volume **7**, Number **3**, June **2014**

doi:10.3934/dcdss.2014.7.543

pp. **543–556**

FREE–CONGESTED AND MICRO–MACRO DESCRIPTIONS OF TRAFFIC FLOW

Francesca Marcellini

Università di Milano-Bicocca
Dipartimento di Matematica e Applicazioni
Via Cozzi 53, 20125 Milano, Italy

Abstract. We present two frameworks for the description of traffic, both consisting in the coupling of systems of different types. First, we consider the Free–Congested model [7, 11], where a scalar conservation law is coupled with a 2×2 system. Then, we present the coupling of a micro- and a macroscopic models, the former consisting in a system of ordinary differential equations and the latter in the usual LWR conservation law, see [10]. A comparison between the two different frameworks is also provided.

1. **Introduction.** We consider mixed systems in the description of dynamics of traffic flow: two different frameworks, both consisting in the coupling of systems of different types, both displaying 2 phases.

The first one is the Free–Congested model, see [11], a macroscopic model displaying 2 phases, *Free* and *Congested*, based on a non-smooth 2×2 system of conservation laws.

To construct this model, recall at first the classical Lighthill-Whitham [23] and Richards [24] (LWR) traffic model

$$\partial_t \rho + \partial_x (\rho V) = 0 \tag{1}$$

which is a scalar conservation law, where $\rho = \rho(t,x)$ is the (mean) traffic density and $V = V(\rho)$ is the (mean) traffic speed. Next we extend the LWR model with two assumptions on the speed V. At first, we assume that, at a given density, different drivers may differ in their *maximal* speed w, so that $V = w\,\psi(\rho)$, with $w \in [\check{w}, \hat{w}]\,, \check{w} > 0$. The function ψ describes the attitude of drivers to choose their speed depending on the traffic density at their location and the maximal speed w is a specific feature of every single driver. Thus we are lead to study the system:

$$\begin{cases} \partial_t \rho + \partial_x(\rho v) = 0 \\ \partial_t w + v\,\partial_x w = 0 \end{cases} \qquad \text{with} \qquad v = w\,\psi(\rho)\,. \tag{2}$$

The role of the second equation above is to let the maximal velocity w be propagated with the traffic speed. We identify the different behaviors of the different drivers by means of their maximal speed, see also [5, 6].

2010 *Mathematics Subject Classification.* 35L65, 90B20.

Key words and phrases. Traffic models, hyperbolic systems of conservation laws, macroscopic traffic models, ordinary differential equations, microscopic traffic models.

The second assumption on the speed is the introduction of a uniform bound, a constant $V_{\max}$ that the drivers do not exceed. We obtain the following model:

$$\begin{cases} \partial_t \rho + \partial_x(\rho v) = 0 \\ \partial_t w + v\,\partial_x w = 0 \end{cases} \qquad \text{with} \qquad v = \min\left\{V_{\max},\, w\,\psi(\rho)\right\}. \tag{3}$$

The above quasilinear system is not in conservation form, so similarly to [18, formula (1)], [2, formula (3.1)], [3, formula (2.2)], [21, formula (1)], [25], we choose to reformulate (3) in conservation form, as follows:

$$\begin{cases} \partial_t \rho + \partial_x\left(\rho\, v(\rho,\eta)\right) = 0 \\ \partial_t \eta + \partial_x\left(\eta\, v(\rho,\eta)\right) = 0 \end{cases} \qquad \text{with} \qquad v(\rho,\eta) = \min\left\{V_{\max}, \frac{\eta}{\rho}\,\psi(\rho)\right\}; \tag{4}$$

see the Remark 1 for some comments on this choice. This model consists of a 2×2 system of conservation laws with a $\mathbf{C^{0,1}}$ but not $\mathbf{C^1}$ flow. Note in fact that $\frac{\eta}{\rho} = w \in [\check{w}, \hat{w}]$.

The second traffic flow model that we present here is the Micro–Macro model, see [10], consisting of a macroscopic and a microscopic descriptions glued together. The macroscopic part is described through the Lighthill–Whitam [23] and Richards [24] model (LWR), that we recall again

$$\partial_t \rho + \partial_x\left(\rho\, v\right) = 0 \tag{5}$$

given by a scalar conservation law. Microscopic models for vehicular traffic consist of a finite set of ordinary differential equations, describing the motion of each vehicle in the traffic flow. Below we consider a first order Follow–the–Leader (FtL) model, where each driver adjusts his/her velocity to the vehicle in front, that is

$$\dot{p}_i = v\left(\frac{\ell}{p_{i+1} - p_i}\right). \tag{6}$$

Here, $p_i = p_i(t)$ is the position of the i-th driver, for $i = 1, \dots, n$, and $p_{i+1} - p_i \geq \ell$ for all $i = 1, \dots, n-1$, the fixed parameter ℓ denoting the (mean) vehicles' length. Here, $\ell/(p_{i+1} - p_i)$ is the local traffic density seen by the driver p_i. Equation (6) needs to be closed with the trajectory of the first driver p_n. Throughout, we carefully select assumptions allowing us to prove that all speeds are bounded.

Our aim is to consider a general situation in which the two descriptions (5) and (6) are alternatively used in different segments of the real line, because the point of cohesion of the two descriptions is not fixed. A similar approach to traffic modeling is in [20], where the model in [2, 26] plays the role here played by the LWR one. See also [12] for the case $n = 1$.

The paper is organized as follows: in the next section we present the Free–Congested description and we study the Riemann Problem for (4). This model is also compared with other models of the same type in the current literature, as well as with a kinetic one. Moreover, we establish a rigorous connection between a *microscopic follow-the-leader* model based on ordinary differential equations and this *macroscopic continuum* model. In Section 3 we present the Micro–Macro description; in particular we treat separately the LWR-FtL case, when the LWR model describes the traffic dynamics on the right and the FtL on the left, and the opposite case, the FtL-LWR one. Moreover some numerical results complete the study of the model. In the last section is also provided a comparison between the two different frameworks, the Free–Congested and the Micro–Macro descriptions, both displaying traffic models with 2 phases.

2. **Free–Congested description.** In this section we present the Free–Congested Model and the main result is the Riemann Problem for (4). We assume at first the following hypotheses:

a. $R, \check{w}, \hat{w}, V_{\max}$ are positive constants, with $\check{w} < \hat{w}$.
b. $\psi \in C^2\left([0,R];[0,1]\right)$ is such that

$$\begin{array}{rclcrcl} \psi(0) & = & 1, & & \psi(R) & = & 0, \\ \psi'(\rho) & \leq & 0, & \dfrac{d^2}{d\rho^2}\left(\rho\,\psi(\rho)\right) & \leq & 0 & \text{for all } \rho \in [0,R]\,. \end{array}$$

c. $\check{w} > V_{\max}$.

Here, R is the maximal possible density; $\check{w}$, respectively $\hat{w}$, is the minimum, respectively maximum, of the maximal speeds of each vehicle; $V_{\max}$ is the overall uniform upper bound on the traffic speed. At **b.**, the first three assumptions on Ψ are the classical conditions usually assumed on speed laws, while the fourth one is technically necessary in the proof of Theorem 2.1, see [11, Section 5]. The latter condition **c.** means that all drivers do feel the presence of the speed limit.

The model in (4) is a macroscopic model displaying 2 phases, the *Free* and the *Congested* phases, defined in the following way:

$$\begin{aligned} F &= \{(\rho, w) \in [0,R] \times [\check{w}, \hat{w}] \colon v(\rho, \rho w) = V_{\max}\} \\ C &= \{(\rho, w) \in [0,R] \times [\check{w}, \hat{w}] \colon v(\rho, \rho w) = w\,\psi(\rho)\} \end{aligned} \tag{7}$$

The phases are presented in Figure 1. Note that F is 1–dimensional in the $(\rho, \rho v)$

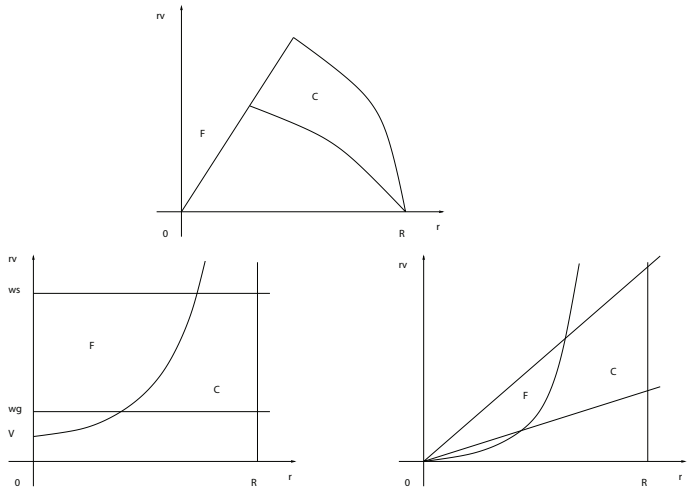

FIGURE 1. The phases F and C in the coordinates $(\rho, \rho v)$, (ρ, w) and (ρ, η). F is 1–dimensional in the $(\rho, \rho v)$ plane, while it is 2–dimensional in the (ρ, w) and (ρ, η) coordinates.

plane of the fundamental diagram, above, while it is 2–dimensional in the (ρ, w) and (ρ, η) coordinates. The representation in coordinates (ρ, η) is technically necessary in the proof of Theorem 2.1, see [11, Section 5]. Note also that both the phases F and C are closed sets and $F \cap C \neq \emptyset$.

The main result is the Riemann Problem for (4).

Theorem 2.1. *Under the assumptions* **a.**, **b.** *and* **c.**, *for all states* (ρ^l,η^l), $(\rho^r,\eta^r)\in F\cup C$, *the Riemann problem consisting of (4) with initial data*

$$\rho(0,x)=\begin{cases}\rho^l & \text{if } x<0\\ \rho^r & \text{if } x>0\end{cases}\qquad \eta(0,x)=\begin{cases}\eta^l & \text{if } x<0\\ \eta^r & \text{if } x>0\end{cases} \tag{8}$$

admits a unique self similar weak solution $(\rho,\eta)=(\rho,\eta)(t,x)$ *constructed as follows:*

(1) If $(\rho^l,\eta^l),(\rho^r,\eta^r)\in F$, *then*

$$(\rho,\eta)(t,x)=\begin{cases}(\rho^l,\eta^l) & \text{if } x<V_{\max}t\\ (\rho^r,\eta^r) & \text{if } x>V_{\max}t\,.\end{cases} \tag{9}$$

(2) If $(\rho^l,\eta^l),(\rho^r,\eta^r)\in C$, *then* (ρ,η) *consists of a* 1*–Lax wave (shock or rarefaction) between* (ρ^l,η^l) *and* (ρ^m,η^m), *followed by a* 2*–contact discontinuity between* (ρ^m,η^m) *and* (ρ^r,η^r). *The middle state* (ρ^m,η^m) *is in* C *and is uniquely characterized by the two conditions* $\eta^m/\rho^m=\eta^l/\rho^l$ *and* $v(\rho^m,\eta^m)=v(\rho^r,\eta^r)$.

(3) If $(\rho^l,\eta^l)\in C$ *and* $(\rho^r,\eta^r)\in F$, *then the solution* (ρ,η) *consists of a rarefaction wave separating* (ρ^r,η^r) *from a state* (ρ^m,η^m) *and by a linear wave separating* (ρ^m,η^m) *from* (ρ^l,η^l). *The middle state* (ρ^m,η^m) *is in* $F\cap C$ *and is uniquely characterized by the two conditions* $\eta^m/\rho^m=\eta^r/\rho^r$ *and* $v(\rho^m,\eta^m)=V$.

(4) If $(\rho^l,\eta^l)\in F$ *and* $(\rho^r,\eta^r)\in C$, *then* (ρ,η) *consists of a shock between* (ρ^l,η^l) *and* (ρ^m,η^m), *followed by a contact discontinuity between* (ρ^m,η^m) *and* (ρ^r,η^r). *The middle state* (ρ^m,η^m) *is in* C *and is uniquely characterized by the two conditions* $\eta^m/\rho^m=\eta^l/\rho^l$ *and* $v(\rho^m,\eta^m)=v(\rho^r,\eta^r)$.

(If $\frac{d^2}{d\rho^2}\left(\rho\,\psi(\rho)\right)$ vanishes, then the words *"shock"* and *"rarefaction"* above have to be understood as *"contact discontinuities").*

For the proof see [11, Section 5].

We also pass from the solution to a single Riemann problem to the properties of the *Riemann Solver*, i.e. of the map $\mathcal{R}\colon (F\cup C)^2\to \mathbf{BV}(\mathbb{R};C\cup F)$ such that $\mathcal{R}\left((\rho^l,\eta^l),(\rho^r,\eta^r)\right)$ is the solution to (4)–(8) computed at time, say, $t=1$. For technical details see [11, Proposition 2.3].

Remark 1. Note that the system (3) is not in conservation form. So we choose to reformulate this quasilinear system in conservation form, as in (4). For smooth solutions, system (3) it is equivalent to infinitely many 2×2 systems of conservation laws. Indeed, introduce a strictly monotone function $f\in\mathbf{C^2}\left([\check w,\hat w];]0,+\infty[\right)$. Then, elementary computations show that, as long as smooth solutions are concerned, system (3) is equivalent to

$$\begin{cases}\partial_t\rho+\partial_x\left(\rho\,\psi(\rho)\,g(\eta/\rho)\right)=0\\ \partial_t\eta+\partial_x\left(\eta\,\psi(\rho)\,g(\eta/\rho)\right)=0\end{cases}\qquad\text{where}\qquad\begin{array}{l}\eta=\rho\,f(w)\text{ and}\\ g\left(f(w)\right)=w\end{array} \tag{10}$$

Clearly, different choices of f yield different weak solutions to (10), but they are all equivalent when written in terms of ρ and w. Thus system (3) is equivalent to (4).

2.1. **Other macroscopic models.** This paragraph is devoted to compare the Free–Congested macroscopic model (4) with others in the current literature. The evolution described by the present model (4) and the corresponding invariant domain depends on the function ψ and on the parameters $V_{\max}$, R, $\check w$ and $\hat w$. Thus we consider differences in the number of free parameters and functions, in the fundamental diagram and in the qualitative structures of the solutions. The fundamental diagram of (4) is in Figure 2.

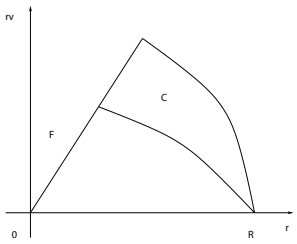

FIGURE 2. The fundamental diagram of the Free–Congested macroscopic model (4).

Consider at first the LWR model in (1). Here, a suitable speed law has to be selected, analogous to the choice of ψ in (4). Moreover, in (4) we also have to set $V_{\max}$, R and the two geometric positive parameters $\check{w}$ and $\hat{w}$.

As long as the data are in F, the solutions to (4) are essentially the same as those of the LWR model (1). In the congested phase, the solutions to (4) obviously present a richer structure, for they generically contain 2 waves instead of 1. The fundamental diagram of (4), shown in Figure 2, seems to better agree with the classical experimental data than that of (1), in Figure 3, left. For the experimental data see Figure 6, in the last section.

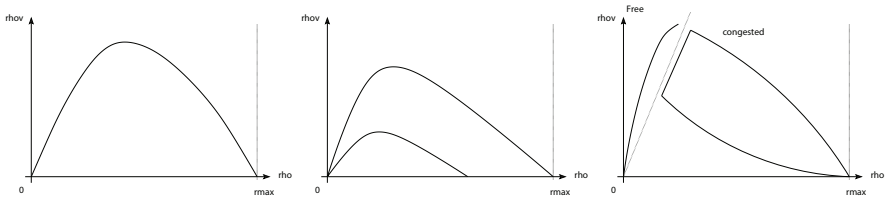

FIGURE 3. Fundamental diagrams, from left to right, of the (LWR) model (1), of the (AR) model (11) and of the 2-phase model (12).

Note also that if in (4) the two geometric parameters $\check{w}$ and $\hat{w}$ coincide, then we recover the LWR (1) model with $V(\rho) = \min\{V_{\max}, \hat{w}\,\psi(\rho)\}$.

Next we want to compare the Free–Congested macroscopic model (4) with the 2×2 Aw–Rascle (AR) model:

$$\begin{cases} \partial_t \rho + \partial_x \left[\rho\, v(\rho, y)\right] = 0 \\ \partial_t y + \partial_x \left[y\, v(\rho, y)\right] = 0 \end{cases} \qquad v(\rho, y) = \frac{y}{\rho} - p(\rho) \tag{11}$$

introduced in [2] and successively refined in several papers, see for instance [1, 4, 14].

The original (AR) model does not distinguish between a free and a congested phase. However, it was extended to a model with phase transition in [14], by the coupling of the LWR model and [2].

In the (AR) model, R and the function $p(\rho)$ need to be selected, similarly to R and ψ in (4). An invariant domain for (11) is the following:

$$\{(\rho, y)\colon \rho \in [0, R] \text{ and } y \in [\rho\,(v_- + p(\rho))\,, \rho\,(v_- + p(\rho))]\}$$

and depends on the speeds v_- and v_+. See the fundamental diagram in Figure 3, center. Thus the definition of an invariant domain requires two parameters, with a role similar to that of $\check{w}$ and $\hat{w}$. Moreover recent versions of (11) contain also a

suitable relaxation source term in the hand side of the second equation; in this case one more arbitrary function needs to be selected. The fundamental diagram of (4), shown in Figure 2, seems to better agree with the classical experimental data than that of the (AR) model, in Figure 3, left. For the experimental data see Figure 6, in the last section.

A qualitative difference between the (AR) model and the present one is that solutions to (11) may well have zero speed while being at a density strictly lower than the maximal one.

From the analytical point of view, the Riemann problem for the (AR) model suffers lack of continuous dependence at vacuum, see [2, Section 4]. However, existence of solutions attaining also the vacuum state was proved in [15], while the 2-phase construction in [14] also displays continuous dependence.

Note also that w in (4) plays a role analogous to that of $v + p\,(\rho)$ in (11).

Consider next the hyperbolic two–phase model presented in [8]:

$$\begin{array}{ll} \text{Free flow: } (\rho,q)\in F, & \text{Congested flow: } (\rho,q)\in C,\\ \partial_t\rho+\partial_x\left[\rho\cdot v_F(\rho)\right]=0, & \left\{\begin{array}{l}\partial_t\rho+\partial_x\left[\rho\cdot v_C(\rho,q)\right]=0\\ \partial_t q+\partial_x\left[(q-q_*)\cdot v_C(\rho,q)\right]=0\end{array}\right.\\ v_F(\rho)=\left(1-\frac{\rho}{R}\right)\cdot V & v_C(\rho,q)=\left(1-\frac{\rho}{R}\right)\cdot\frac{q}{\rho}\end{array} \tag{12}$$

The notation is very similar to the present one: there are two distinct phases as in (4). In the theory of hyperbolic conservation laws models showing phase transitions as (12), in terms of traffic flows correspond to two distinct behaviors, *Free* or *Congested*. In (12) the phases are defined as:

$$F=\{(\rho,q)\in[0,R]\times\Re^+\colon v_f(\rho)\geq V_f,\ q=\rho\cdot V\},$$
$$C=\left\{(\rho,q)\in[0,R]\times\Re^+\colon v_c(\rho.q)\leq V_c,\ \frac{q-q_*}{\rho}\in\left[\frac{Q_1-q_*}{R},\frac{Q_2-q_*}{R}\right]\right\}.$$

The evolution in (12) depends on the parameters V, R and q_* and also the invariant domains F and C depend on V_f, V_c, Q_1 and Q_2.

Note that in both models, as well as in that presented in [14], the free phase is one dimensional, while the congested phase is bidimensional. This is in agreement with the experimental data, see Figure 6 in the last section.

The main difference between fundamental diagrams of (12), see Figure 3, right, and that of (4) in Figure 2, is that in (12) the two phases are *disconnected*: there is a *gap* between the free and the congested phase. This restriction is necessary for the well posedness of the Riemann problem for (12) and can be hardly justified on the basis of experimental data. More recently, the global well-posedness of the model (12) was proved in [9].

2.2. **A kinetic model.** In this paragraph we want to compare the Free–Congested model in (4) with the following kinetic model:

$$\partial_t r(t,x;w)+\partial_x\left[w\,r(t,x;w)\,\psi\left(\int_{\check{w}}^{\hat{w}} r(t,x;w')\,dw'\right)\right]=0\,. \tag{13}$$

This model is an n-population generalization of the Lighthill-Whitham and Richards traffic flow model, introduced in [6, Section 1]. In general, in the kinetic models is defined a function $f=f(t,x,V)$ which expresses the probability of having a vehicle at time t in position x which runs with velocity V. Above, the function $r=r(t,x;w)$ is the probability density of vehicles having maximal speed w that at

time t are at point x. In (13), the function ψ and the maximal speed w play the same role as in (4).

From the analytical point of view, the existence of solutions to (13) has not been proved, yet. The main result in [6] only states that (13) can be rigorously obtained as the limit of systems of $n \times n$ conservation laws describing n populations of vehicles, each characterized by their maximal speed.

In (13) ψ is the function to be specified, as in (4). Moreover the parameter R (which is normalized to 1 in [6]), $\check{w}$ and $\hat{w}$, are similarly to those in (4). Since no limit speed is there defined, no parameter in (13) has the same role as here $V_{\max}$.

Being of a kinetic nature, there is no real equivalent to a fundamental diagram for (13).

Next we want to establish a connection between the Free–Congested Model and the kinetic one. Let the measure r solve (13) and be such that for suitable functions ρ and w

$$r(t,x;\cdot) = \rho(t,x)\,\delta_{w(t,x)} \tag{14}$$

where δ is the usual Dirac measure. Then, formally, (ρ, w) solves (4). Indeed, for the first equation simply substitute (14) in (13) and integrate; for the second equation substitute (14) in (13), multiply by w and integrate over $[\check{w}, \hat{w}]$. Formally, (ρ, w) solves (4) when $v(\rho,\eta) = \frac{\eta}{\rho}\psi(\rho)$ since no parameter in (13) has the same role as here $V_{\max}$.

2.3. **Micro–Macro limit.** In this paragraph we want to establish a connection between the Free–Congested Model and a Follow-the-Leader Model, based on ordinary differential equations. See [1] for a different approach. In contrast to the above reference, we establish *directly* a connection between the two models without viewing both systems as issued from a same fully discrete system (Godunov scheme) with different limits, and without passing in Lagrangian coordinates.

The macroscopic description and the microscopic one are related through *particle paths*, which are the trajectories of single individuals, namely the solutions to the ordinary differential equations. According to (3), a single driver starting from $\tilde{p}$ at time $t = 0$ follows the following particle path $p = p(t)$,

$$\begin{cases} \dot{p} = v\left(\rho\left(t, p(t)\right), w\left((t, p(t))\right)\right) \\ p(0) = \tilde{p} \end{cases} \qquad v(\rho, w) = \min\left\{V_{\max},\, w\,\psi(\rho)\right\}. \tag{15}$$

Refer to [12] for the well posedness of the particle path for the LWR model.

Recall now that the maximal speed w is a specific feature of every single driver, a Lagrangian marker, i.e. for all $\tilde{p}$:

$$w\left(t, p(t)\right) = w(0, \tilde{p}).$$

On the other hand, we have to approximate ρ. From a microscopic point of view, if the drivers are distributed along the road, then ρ is approximated by $\ell/(p_{i+1} - p_i)$, where ℓ is a standard length of a car.

We fix $L > 0$ and assume that $n+1$ drivers are distributed along $[-L, L]$. Then, the natural microscopic counterpart to (4) is therefore the *follow-the-leader* (FTL) model defined by the following Cauchy problem:

$$\begin{cases} \dot{p}_i = v\left(\frac{\ell}{p_{i+1} - p_i}, w_i\right) & i = 1, \dots, n \\ \dot{p}_{n+1} = V_{\max} & \\ p_i(0) = \tilde{p}_i & i = 1, \dots, n+1 \end{cases} \tag{16}$$

where $p_1, ..., p_{n+1}$ are the positions of the $n+1$ drivers, $\tilde{p}_1 = -L$ and $\tilde{p}_{n+1} = L - l$.

The following Proposition 1 shows that the Cauchy problem (16) admits a unique global solution defined for every $t \geq 0$ and such that $p_{i+1} - p_i \geq \ell$ for $i = 1, \dots, n$ and for all $t \geq 0$.

Proposition 1. *Let* ***a.***, ***b.*** *and* ***c.*** *hold. Fix $L > 0$. For any $n \in \mathbb{N}$, with $n \geq 3$, choose initial data $\tilde{p}_i^n$ for $i = 1, \dots, n$ satisfying $\tilde{p}_{i+1}^n - \tilde{p}_i^n \geq \ell$. Then, the Cauchy problem (16) admits a unique solution $p_i^n = p_i^n(t)$, for $i = 1, \dots, n+1$, defined for all $t \geq 0$ and satisfying $p_{i+1}^n(t) - p_i^n(t) \geq \ell$ for all $t \geq 0$ and for $i = 1, \dots, n$.*

For the proof see [11, Section 5].

Our next aim is to rigorously show that as $n \to +\infty$, that is as the number of the vehicles increases to infinity, with $n\,l = \text{constant} > 0$, the microscopic model in (16) yields the macroscopic one in (4). The limit establishes a connection between the two classes of models.

Given the position p^i of every single vehicle and its maximal speed w_i, for $i = 1, \dots, n+1$, the macroscopic variables ρ, w are given by

$$\rho(x) = \sum_{i=1}^{n} \frac{\ell}{p_{i+1}^n - p_i^n}\, \chi_{[p_i^n, p_{i+1}^n[}(x) \quad \text{and} \quad w(x) = \sum_{i=1}^{n} w_i^n\, \chi_{[p_i^n, p_{i+1}^n[}(x)\,.$$

Note that necessarily $p_{i+1}^n - p_i^n \geq \ell$ for $i = 1, \dots, n$.

On the contrary, given the macroscopic variables $(\rho, w) \in (\mathbf{L^1} \cap \mathbf{BV})(\mathbb{R}; [0,1] \times [\check{w}, \hat{w}])$, with $\operatorname{supp} \rho$, $\operatorname{supp} w \subseteq [-L, L]$, we reconstruct the following microscopic description;

$$\begin{aligned}
\ell &= \left(\int_{\mathbb{R}} \rho(x)\, dx \right) / n \\
p_{n+1}^n &= L - \ell \\
p_i^n &= \max \left\{ p \in [-L, L] \colon \int_p^{p_{i+1}} \rho(x)\, dx = \ell \right\} \quad \text{for } i = 1, \dots, n \\
w_i^n &= w(p_i^n +) \quad \text{for } i = 1, \dots, n+1\,.
\end{aligned}$$

Note that $\int_{\mathbb{R}} \rho(x)\, dx = n\ell > 0$.

Now we are able to rigorously show that, as the number of vehicles increases to infinity, the microscopic model in (16) yields the macroscopic one in (4).

Proposition 2. *Let* ***a.***, ***b.*** *and* ***c.*** *hold. Fix $T > 0$. Choose $(\tilde{\rho}, \tilde{w}) \in (\mathbf{L^1} \cap \mathbf{BV})(\mathbb{R}; [0,1] \times [\check{w}, \hat{w}])$ with $\operatorname{supp} \tilde{\rho}$, $\operatorname{supp} \tilde{w} \subseteq [-L, L]$. Construct the initial data for the microscopic model setting $\ell = \left(\int_{\mathbb{R}} \tilde{\rho}(x)\, dx \right) / n$ and*

$$\begin{aligned}
\tilde{p}_{n+1}^n &= L - \ell \\
\tilde{p}_i^n &= \max \left\{ p \in [-L, L] \colon \int_p^{\tilde{p}_{i+1}} \tilde{\rho}(x)\, dx = \ell \right\} \quad \textit{for } i = 1, \dots, n \\
\tilde{w}_i^n &= \tilde{w}(p_i^n +) \quad \textit{for } i = 1, \dots, n+1\,.
\end{aligned}$$

Let $p_i^n(t)$, for $i = 1, \dots, n$, be the corresponding solution to (16). Define

$$\rho^n(t,x) = \sum_{i=1}^{n} \frac{\ell}{p_{i+1}^n(t) - p_i^n(t)}\, \chi_{[p_i^n(t), p_{i+1}^n(t)[}(x) \tag{17}$$

$$w^n(t,x) = \sum_{i=1}^{n} \tilde{w}_i^n\, \chi_{[p_i^n(t), p_{i+1}^n(t)[}(x)\,. \tag{18}$$

If there exists a pair $(\rho, w) \in \mathbf{L}^\infty\big([0,T];\mathbf{L^1}(\mathbb{R};[0,1]\times[\check{w},\hat{w}])\big)$ *such that*

$$\lim_{n\to+\infty}(\rho^n, w^n)(t,x) = (\rho, w)(t,x) \qquad p.a.e.$$

then, the pair $(\rho, \rho w)$ *is a weak solution to (4) with initial datum* $(\tilde{\rho}, \tilde{\rho}\tilde{w})$.

For the proof see [11, Section 5].

3. **Micro–Macro description.** In this section we present a traffic model consisting of a gluing between the Lighthill-Whitham and Richards macroscopic model with a first order microscopic follow the leader model.

Our aim is to consider a general situation, in which the two descriptions (5) and (6) are alternatively used in different segments of the real line. This is because the point of cohesion of the two frameworks is not fixed, extending the approach presented in [20]. The general case is presented in [10].

Below, we give some notations and a well posedness result separately for the LWR-FtL case, when the LWR model describes the traffic dynamics on the right and the FtL on the left, and for the opposite case, the FtL-LWR one.

Throughout, we denote $\mathbb{R}^+ = [0,+\infty[$ and $\mathring{\mathbb{R}}^+ =]0,+\infty[$. For any $n \in \mathbb{N}$ and $\ell \in \mathring{\mathbb{R}}^+$, the set of admissible positions of n vehicles of length ℓ is

$$\mathcal{P}^n_\ell = \{p \in \mathbb{R}^n \colon p_{i+1} - p_i \geq \ell \text{ for } i = 1,\dots,n-1\}\ . \tag{19}$$

We assume the following condition on the speed law:

(v): $v \in \mathbf{C^2}([0,1];\mathbb{R}^+)$ is strictly decreasing, with $v(1) = 0$ and is such that $\frac{d^2}{d\rho^2}\left(\rho\, v(\rho)\right) < 0$.

3.1. **The case LWR-FtL.** Let n vehicles start at time $t = 0$ from positions $\bar{p} \in \mathcal{P}^n_\ell$ and use the LWR model to describe the traffic dynamics for $x < \bar{p}_1$. The system is the following:

$$\begin{cases} \partial_t\rho + \partial_x\left(\rho\, v(\rho)\right) = 0 & t \in \mathbb{R}^+ & \text{and } x < p_1(t) \\ \dot{p}_i = v\left(\frac{\ell}{p_{i+1}-p_i}\right) & t \in \mathbb{R}^+ & \text{and } i = 1,\dots,n-1 \\ \dot{p}_n = w(t) & t \in \mathbb{R}^+ & \\ \rho(0,x) = \bar{\rho}(x) & x \leq \bar{p}_1 & \\ p(0) = \bar{p} & & \end{cases} \tag{20}$$

where $w \in \mathbf{L}^\infty(\mathbb{R}^+;\mathbb{R}^+)$ is the speed of the first driver, that is the leader, $\bar{\rho} \in (\mathbf{L^1}\cap\mathbf{BV})(\mathbb{R};[0,1])$ describes the vehicles' distribution for $x < \bar{p}_1$ and $\bar{p} \in \mathcal{P}^n_\ell$. In system (20), the trajectory of p_1 acts as a boundary between the microscopic model on its right and the macroscopic one on its left.

A solution to (20) on the time interval $[0,T[$, consists of map

$$\begin{aligned} \rho &\in \mathbf{C^0}\left([0,T];(\mathbf{L^1}\cap\mathbf{BV})(\mathbb{R};[0,1])\right) \qquad \text{with } \rho(t,x) = 0 \text{ whenever } x < p_1(t) \\ p &\in \mathbf{W^{1,\infty}}([0,T];\mathbb{R}^n). \end{aligned}$$

The following result holds:

Proposition 3. *Fix* $\ell > 0$, $V > 0$, $n \in \mathbb{N}$ *with* $n \geq 2$ *and a* v *that satisfies* ***(v)****. Let* w *be in* $\mathbf{L}^\infty(\mathbb{R}^+;[0,V])$. *For any* $\bar{p} \in \mathcal{P}^n_\ell$ *and for any* $\bar{\rho} \in (\mathbf{L^1}\cap\mathbf{BV})(\mathbb{R};[0,1])$, *problem (20) admits a unique solution.*

For the proof see [10].

3.2. **The case FtL-LWR.** Next let n vehicles start at time $t = 0$ from positions $\bar{p} \in \mathcal{P}_\ell^n$ and use the LWR model to describe the traffic dynamics for $x > p_n(t)$. Now the free boundary between the two models is the trajectory $p_n = p_n(t)$, chosen so that $\dot{p}_n = v\left(\rho(t, p_n(t))\right)$. We have the following system:

$$\begin{cases} \partial_t \rho + \partial_x \left(\rho\, v(\rho)\right) = 0 & t \in \mathbb{R}^+ & \text{and } x > p_n(t) \\ \dot{p}_i = v\left(\frac{\ell}{p_{i+1} - p_i}\right) & t \in \mathbb{R}^+ & \text{and } i = 1, \dots, n-1 \\ \dot{p}_n = v\left(\rho(t, p_n(t))\right) & t \in \mathbb{R}^+ & \\ \rho(0, x) = \bar{\rho}(x) & x \geq \bar{p}_n & \\ p(0) = \bar{p} & & \end{cases} \tag{21}$$

where $\bar{\rho} \in (\mathbf{L^1} \cap \mathbf{BV})(\mathbb{R}; [0,1])$ describes the macroscopic vehicles' distribution for $x > \bar{p}_n$ and $\bar{p} \in \mathcal{P}_\ell^n$ gives the initial positions of the discrete vehicles. In system (21), the trajectory of p_n acts as a boundary between the microscopic model on its left and the macroscopic one on its right.

A solution to (21) on the time interval $[0, T[$, consists of map

$$\begin{aligned} \rho &\in \mathbf{C^0}\left([0,T]; (\mathbf{L^1} \cap \mathbf{BV})(\mathbb{R}; [0,1])\right) \quad \text{with } \rho(t,x) = 0 \text{ whenever } x > p_n(t) \\ p &\in \mathbf{W^{1,\infty}}([0,T]; \mathbb{R}^n). \end{aligned}$$

The following result holds:

Proposition 4. *Fix $\ell > 0$, $V > 0$, $n \in \mathbb{N}$ with $n \geq 2$ and a v that satisfies **(v)**. For any $\bar{p} \in \mathcal{P}_\ell^n$ and for any $\bar{\rho} \in (\mathbf{L^1} \cap \mathbf{BV})(\mathbb{R}; [0,1])$, problem (21) admits a unique solution.*

For the proof see [10].

3.3. **Numerical integrations.** Next we present some numerical results for the two different descriptions discussed above. We use the Lax-Friedrichs algorithm, see [22, Section 12.1], for the partial differential equation and the explicit forward Euler method for the ordinary differential equation.

Concerning the LWR-FtL case we refer to the model in (20), in agreement with the notations in Paragraph 3.1. We choose

$$v(\rho) = 1 - \rho\,, \qquad \ell = 0.49 \qquad \text{and} \qquad w(t) = 0.75 \tag{22}$$

with initial datum

$$\begin{aligned} \bar{\rho}(x) &= \chi_{[-2,-0.5]}(x) + 0.8\chi_{[-6,-5]}(x) + 0.6\chi_{[-9,-8]}(x) \\ \bar{p} &= [0,\ 2,\ 4,\ 6.5,\ 7,\ 7.5,\ 8,\ 8.5,\ 9,\ 9.5]\ . \end{aligned} \tag{23}$$

Note that the above choices are consistent with the assumptions required in Proposition 3. The numerical integration is displayed in Figure 4, in the (t, x) plane. It was computed with a space mesh size $\Delta x = 2.5 \times 10^{-3}$ and a time mesh size updated at each time step so that

$$\Delta t = 0.9 \cdot \Delta x / \Lambda, \tag{24}$$

where Λ is the maximal characteristic speed.

In the macroscopic part, on the left, we have shocks and rarefaction curves which interact each other, which is the typical behavior of the solutions to the LWR model. In the microscopic part, on the right, there are the trajectories of the single vehicles. Due to the choice (23) of the initial datum, the cars in front start very slowly, while the ones in the back start very quickly and then, they have to slow down, because of the cars that they have in front of them, according to (6). This situation causes

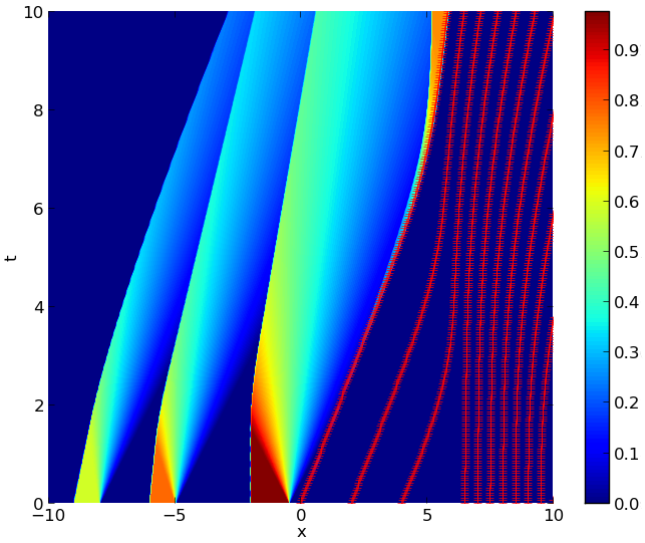

FIGURE 4. Numerical integration of the LWR–FtL model (20), with the the choices (22) and initial datum (23). The interaction between the micro- and macroscopic phases is shown by the shock arising in the macroscopic part at about $t = 4$, fully visible from about $t = 8$.

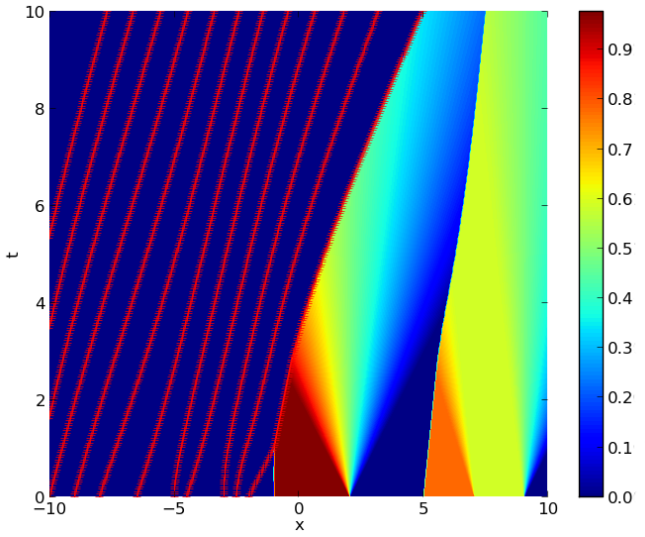

FIGURE 5. Numerical integration of the FtL–LWR model (21), with the the choices (22) and initial datum (25). The LWR density in the interval $[-1, 2]$ is maximal, hence the traffic speed vanishes there. As a consequence, the first vehicle in the microscopic phase reaches the phase boundary at about $t = 1$ and at that time its velocity is discontinuous.

the formation of a shock on the macroscopic part, which arises about at time $t = 4$, behind the leftmost driver, and is fully visible about from $t = 8$.

For the opposite case, the FtL-LWR one, we refer to the model in (21). We keep using the choices (22), but with the initial datum

$$\begin{array}{rcl} \bar\rho(x) & = & \chi_{[-1,2]}(x) + 0.8\chi_{[5,7]}(x) + 0.6\chi_{[7,9]}(x) \\ \bar p & = & [-11.5, -11, -10.5, -10, -9, -8, -6.5, -5, -4.5, -3, -2.5, -2] \end{array} \tag{25}$$

with a mesh $\Delta x = 10^{-3}$ and a time mesh chosen as in (24). The FtL-LWR case is presented in Figure 5, where it is shown a collision between the micro- and macroscopic models. The LWR density in the interval $[-1, 2]$ is maximal and hence the traffic speed vanishes in the same interval. As a consequence, the first driver in the microscopic part reaches the phase boundary at about $t = 1$ and at that time its velocity suffers a discontinuity.

Figure 4 and Figure 5 explain how the two micro- and macroscopic models coexist in a single model. There is an exchange of information, which is propagated back, between the two diferent descriptions but there isn't an exchange of mass.

4. **Two–Phase models.** The Free–Congested and the Micro–Macro descriptions, both consist in the coupling of systems of different types and both display traffic models with 2 phases.

The Free–Congested model, described in Section 2, is a *Two–Phase model* based on a non-smooth 2×2 system of conservation laws. The assumptions on the speed in (3) provide the formation of two distinct phases: the *Free* and the *Congested* phases.

The Micro-Macro model, described in Section 3, is another *Two–Phase model*. Two different descriptions coexist in a single model: the LWR modelizes the continuum traffic dynamics and the FtL describes the motion of each vehicle in traffic flow.

The Free–Congested case as well as the Micro-Macro one are "free boundary" models, with edges of phases to be determined.

Several observations of traffic flow can be modelized in two different behaviors, sometimes called *phases*, see [8, 11, 13, 14, 17]. At low density and high speed, the flow appears to be reasonably described by a function of the (mean) traffic density. On the contrary, at high density and low speed, flow appears not to be a single valued function of the density.

The Free–Congested model provides an explanation of this phenomenon and the resulting fundamental diagram is very similar to the experimental ones usually observed in the literature. Indeed, compare the graphs in Figure 6 with the fundamental diagram of the Free–Congested model in Figure 2.

One of the major difficulties in the treatment of the Free–Congested model has been the study of phase transitions, see also [7, 8, 9, 11, 14]. In this model a vehicle can enter in or exit from one of the two distinct phases, depending on the traffic conditions. This does not occur in the Micro-Macro model: there isn't an exchange of mass. A vehicle in the microscopic phase will always remain in the microscopic phase and similarly a vehicle in the macroscopic phase will always remain in the macroscopic phase. The numerical results explained in Paragraph 3.3 show this feature. Indeed both Figure 4 and Figure 5 explain how the two micro- and macroscopic frameworks coexist in a single model, although being separated.

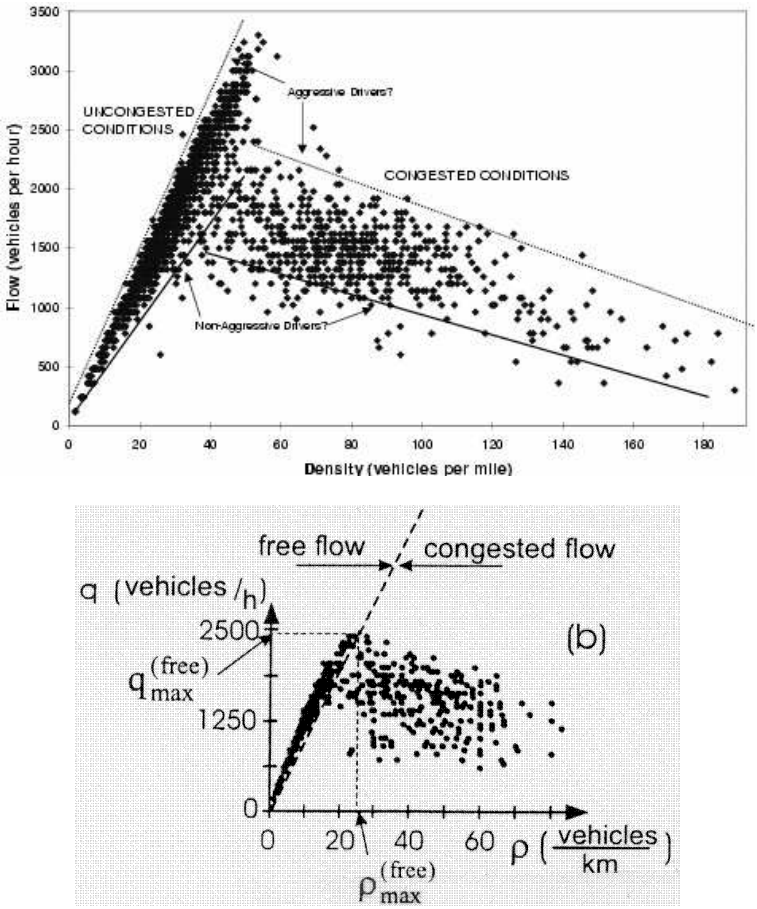

FIGURE 6. Classical experimental fundamental diagrams. Top, [19, Figure 1] and, bottom, [17, Figure 1], (see also [16]).

Note in fact that there is an exchange of information, which is propagated back, between the two different descriptions, but there isn't an exchange of mass.

Acknowledgments. The author would like to thank the funding of ERC, a starting grant funded project for the TRAM3: Traffic Management by Macroscopic Models.

REFERENCES

[1] A. Aw, A. Klar, T. Materne and M. Rascle, Derivation of continuum traffic flow models from microscopic follow-the-leader models, *SIAM J. Appl. Math.*, **63** (2002), 259–278 (electronic).
[2] A. Aw and M. Rascle, Resurrection of "second order" models of traffic flow, *SIAM J. Appl. Math.*, **60** (2000), 916–938 (electronic).
[3] P. Bagnerini, R. M. Colombo and A. Corli, On the role of source terms in continuum traffic flow models, *Math. Comput. Modelling*, **44** (2006), 917–930.
[4] P. Bagnerini and M. Rascle, A multiclass homogenized hyperbolic model of traffic flow, *SIAM J. Math. Anal.*, **35** (2003), 949–973 (electronic).
[5] S. Benzoni Gavage and R. M. Colombo, An n-populations model for traffic flow, *Europ. J. Appl. Math.*, **14** (2003), 587–612.

[6] S. Benzoni-Gavage, R. M. Colombo and P. Gwiazda, Measure valued solutions to conservation laws motivated by traffic modelling, *Proc. R. Soc. Lond. Ser. A Math. Phys. Eng. Sci.*, **462** (2006), 1791–1803.
[7] S. Blandin, D. Work, P. Goatin, B. Piccoli and A. Bayen, A general phase transition model for vehicular traffic, *SIAM J. Appl. Math.*, **71** (2011), 107–127.
[8] R. M. Colombo, Hyperbolic phase transitions in traffic flow, *SIAM J. Appl. Math.*, **63** (2002), 708–721.
[9] R. M. Colombo, P. Goatin and F. S. Priuli, Global well posedness of traffic flow models with phase transitions, *Nonlinear Anal.*, **66** (2007), 2413–2426.
[10] R. M. Colombo and F. Marcellini, A mixed ode-pde model for vehicular traffic, preprint, (2013).
[11] R. M. Colombo, F. Marcellini and M. Rascle, A 2-phase traffic model based on a speed bound, *SIAM J. Appl. Math.*, **70** (2010), 2652–2666.
[12] R. M. Colombo and A. Marson, A Hölder continuous ODE related to traffic flow, *Proc. Roy. Soc. Edinburgh Sect. A*, **133** (2003), 759–772.
[13] L. C. Edie, Car-following and steady-state theory for noncongested traffic, *Operations Res.*, **9** (1961), 66–76.
[14] P. Goatin, The Aw-Rascle vehicular traffic flow model with phase transitions, *Math. Comput. Modelling*, **44** (2006), 287–303.
[15] M. Godvik and H. Hanche-Olsen, Existence of solutions for the Aw-Rascle traffic flow model with vacuum, *J. Hyperbolic Differ. Equ.*, **5** (2008), 45–63.
[16] D. Helbing and M. Treiber, Critical discussion of synchronized flow, *Cooper@tive Tr@nsport@tion Dyn@mics*, **1** (2002).
[17] B. S. Kerner, Phase transitions in traffic flow, in *Traffic and Granular Flow '99*, (eds., D. Helbing, H. Hermann, M. Schreckenberg and D. Wolf), Springer Verlag, 2000, 253–283.
[18] B. L. Keyfitz and H. C. Kranzer, A system of nonstrictly hyperbolic conservation laws arising in elasticity theory, *Arch. Rational Mech. Anal.*, **72** (1979/80), 219–241.
[19] K. M. Kockelman, Modeling traffics flow-density relation: Accommodation of multiple flow regimes and traveler types, *Transportation*, **28** (2001), 363–374.
[20] C. Lattanzio and B. Piccoli, Coupling of microscopic and macroscopic traffic models at boundaries, *Math. Models Methods Appl. Sci.*, **20** (2010), 2349–2370.
[21] J. P. Lebacque, S. Mammar and H. Haj-Salem, Generic second order traffic flow modelling, in *Transportation and Traffic Theory: Proceedings of the 17th International Symposium on Transportation and Traffic Theory*, 2007.
[22] R. J. LeVeque, *Numerical Methods for Conservation Laws*, Second edition, Lectures in Mathematics ETH Zürich, Birkhäuser Verlag, Basel, 1992.
[23] M. J. Lighthill and G. B. Whitham, On kinematic waves. II. A theory of traffic flow on long crowded roads, *Proc. Roy. Soc. London. Ser. A.*, **229** (1955), 317–345.
[24] P. I. Richards, Shock waves on the highway, *Operations Res.*, **4** (1956), 42–51.
[25] B. Temple, Systems of conservation laws with invariant submanifolds, *Trans. Amer. Math. Soc.*, **280** (1983), 781–795.
[26] H. Zhang, A non-equilibrium traffic model devoid of gas-like behavior, *Transportation Research Part B: Methodological*, **36** (2002), 275–290.

Received May 2013; revised July 2013.

E-mail address: francesca.marcellini@unimib.it